J Electr Eng Technol.2017; 12(5): 1925-1933
http://doi.org/10.5370/JEET.2017.12.5.1925

ISSN(Print) 1975-0102
ISSN(Online) 2093-7423

A New Three-Phase Current Modulation Method to Suppress the Commutation Torque Ripple of Brushless DC Motor

Zhiqiang Wang*, Shuai Yin and Tiehua Ma†**

Abstract – The brushless DC motor's commutation torque ripple is caused by inconsistency in the rate of phase current change. Thus, a method that considers armature resistance is proposed to modulate phase current. The three-phase control strategy, which involves the "open-phase conduction, off-phase pulse width modulation, and maintained non-commutation phase" technique, is applied during commutation at full-speed segments of the motor. Changes in each phase current are analyzed theoretically by establishing mathematical model based on phase current to determine the relative difference among shutdown phase, duty, and motor operating parameters. The turn-on and turn-off phase current change rates are made to be consistent to ensure less non-commutation phase current ripple, then the torque ripple is inhibited. The simulation results show that the phase commutation current and torque ripple coefficient of the proposed method are reduced from 56.9% and 55.5% to 6.8% and 6.1%, respectively. In the experiment system, the pulsation coefficient of the motor phase current is reduced from 40.0% to 16.7% at low speed and 50.0% to 18.8% at high speed. The simulation and experimental results show that the proposed control method significantly inhibits commutation current and torque in the full section.

Keywords: Brushless DC motor, Commutation torque ripple, Current control, Armature resistance

1. Introduction

The brushless DC motor(BLDCM) has been extensively applied[1–3] in household, automobile driving, medical, aerospace, industrial automation, and other fields because of its high efficiency, easy operation, high energy density, etc. However, the torque ripple of the motor drive system problem affects the reliability and shorten the life of the system and restrict the application of a BLDCM for cases requiring high-precision, high-stability conditions. In a variety of factors that cause torque ripple of the BLDCM commutation torque ripple is the most important factor. Numerous studies have been conducted to effectively suppress this ripple. Studies have used direct torque control [4-8], considering non-ideal back EMF [9-14], ideal back EMF [15-23] and other methods to suppress commutation torque ripple.

Torque ripple was reduced under non-ideal counter EMF [9-14]. Integral variable structure control, which modulates six power devices, was also used to make the non-commutation phase current track the reference phase current and suppress torque ripple[9]. The establishment of the non-commutation phase current objective function of Finite-state model predictive control to ensure that the phase current is smooth[10-12].The commutation torque ripple of a BLDCM without position sensor was also suppressed using a three-phase PWM modulation [14].

In the ideal trapezoidal back EMF[15-23], a variety of control strategies are used to keep the actual current tracking reference current to ensure that the commutation phase current is smooth and the commutation torque ripple is eliminated. The current during non-commutation can be smooth, and the commutation torque ripple can be reduced when the DC bus voltage is four times as much as the counter electromotive voltage [15]. In [18], a method is proposed to suppress the current ripple during the non-commutation phase by controlling the DC bus voltage. A technique by controlling the commutation phase three-phase current matching modulation to ensure less current pulses during the non-commutation phase is also proposed in [19-20]. A novel space-vector method to control current is used in [21] to suppress the commutation torque ripple. In [23], the commutation process is divided into three functional areas by analyzing the transient and steady state, and each phase is controlled by different PWM currents. The method is relatively simple, and the current during the non-commutation phase is more stable. However, the winding resistance on the commutation torque ripple is ignored in this process. The winding resistance is small, but ignoring the winding resistance will result in about 20% error when the duty ratio is 0.6.

The method in which the back-EMF is considered to suppress torque ripple will increase the cost of the control CPU, making this method unsuitable for low-power control

† Corresponding Author: School of Computer Science and College Engineering, North University of China. (matiehua@nuc.edu.cn)
* School of Computer Science and College Engineering, North University of China. (wangzhiqiangwxdp@hotmail.com)
** College of Mechanical Engineering, Zaozhuang University, China. (yins8866@163.com)
Received: January 13, 2017; Accepted: June 4, 2017

chip. Errors caused by imprecise back-EMF value will introduce higher torque ripple. Therefore, in this study, considering the influence of armature resistance on the commutation phase current and using the back EMF as an ideal trapezoidal back EMF suppress the commutation torque ripple in a BLDCM are investigated. During the full-speed operation of the motor, the high-speed and low-speed zones are ignored, and complex modulation of the commutation current is performed. The results show the rate of decline in current during the off-phase and the rate of increase in current during conduction to stabilize the current during the non-commutation phase. Thus, the commutation torque ripple of a BLDCM is eliminated.

2. Theoretical Analysis

2.1 The reason of torque ripple in a BLDCM

Simultaneous conduction using a two-phase method is frequently applied to maximize the use of winding and obtain higher torque. Two MOSFETs always function under conduction mode. The current flows through a certain phase of the three-phase winding and flows through a certain phase of the other two phases all the way to the ground. The motor commutates once every 60 electrical degrees. The relationship of phase current and EMF are shown in Fig. 1.

During the modulation of the three-phase current, the current during the off-phase slowly increases but rapidly declines when the three-phase winding switches from one phase to another. However, the current during the three-phase winding phase is zero, which will inevitably lead to fluctuations in the current during the non-commutation phase.

Assuming a maximum counter EMF is E, the electromagnetic torque during commutation is calculated as follows [10]:

$$T_e = \left(Ei_a - E\left(i_b + i_c\right)\right)/\omega = -K_T i_c \qquad (1)$$

where K_T is the torque coefficient.

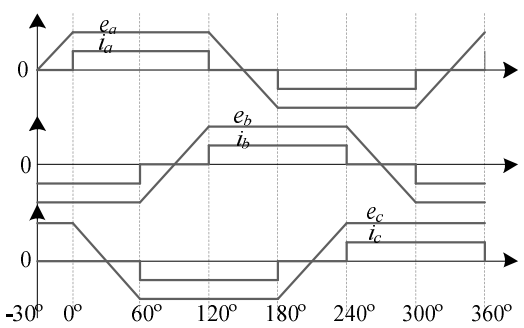

Fig. 1. Waveform of the trapezoidal back-EMF and phase winding current

Thus, the change in current during conduction, commutation, and off-phase times will inevitably lead to inconsistent current during the non-commutation phase, resulting in commutation torque ripple.

In [15], when $U_d > 4E$, the ramp rate during conduction is faster than the decline rate during shutdown in the three-phase winding. The increase in current during the non-commutation phase increases the commutation torque. When $U_d < 4E$, the ramp rate during conduction is slower than the decline rate during shutdown in the three-phase winding. The decrease in current during the non-commutation phase decreases the commutation torque. When $U_d = 4E$, the ramp rate during conduction is equal to the decline rate during shutdown in three-phase winding. In this case, torque remains constant during commutation.

2.2 Proposed method to control commutation current

The PWM-ON method which adjusts speed is still used in the proposed control method during conduction. The "open-phase conduction, off-phase pulse width modulation, and maintained non-commutation phase," which is a smooth commutation control method during commutation is proposed in this paper. The fundamental goal of commutation is to ensure the stability of the current during the non-commutation phase to suppress commutation torque ripple.

The course of change during conduction from *ab* to *ac* as an example to explain the work process is shown. During the *ab* phase conduction, the motor works under conduction mode, power device S_a^+ is chopping, and S_b^- is normally open. The motor commutates when a commutation signal is detected. In this mode, S_a^+ is still chopping at d duty cycle, S_c^- is fully open, and S_b^- is chopping at d_{off} duty cycle. The phase current eventually stabilizes, commutation mode ends, and the motor switches back to conduction mode. In this case, S_a^+ remains fully open, and S_c^- is chopping at d duty cycle. The sequence diagram of the power device is shown in Fig. 2.

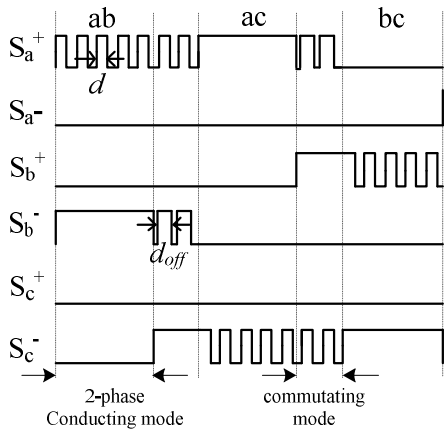

Fig. 2. The power device sequence diagram

2.3 Duty calculation during shutdown

After determining the commutation method, changes in the phase current are analyzed separately in each state of commutation to obtain the duty cycle during the off-phase. The change in conduction phase from *ab* to *ac* is considered as an example. S_a^+ is chopping, while S_b^-, and S_c^- are conducting when the conducting mode switches to commutation mode. Moreover, the bus current starts from the positive power flow through a phase winding shunt to b^- and c^-phase winding. The current flows into the negative power supply. The conducting–winding at the motor commutation moment is shown in Fig. 3 (a). When $T_s \cdot d_{off}$ is the time spent (Note: T_s represents the PWM cycle), S_b^- changes from conduction phase to off-phase, b^- phase winding becomes freewheeling through the freewheeling diode D_b^+, and winding currents are in working mode [Fig. 3(b)].

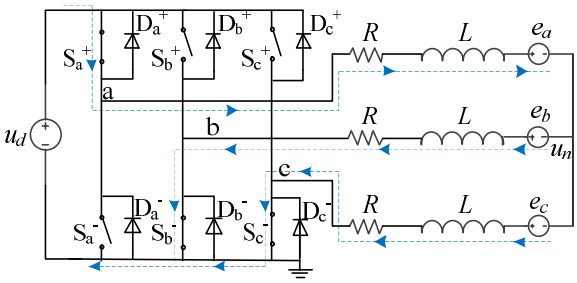

(a) S_b^- turn on

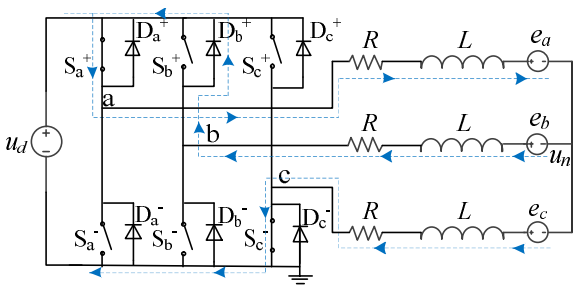

(b) S_b^- turn off

Fig. 3. Three-phase winding conduction of S_b^- turn on and turn off

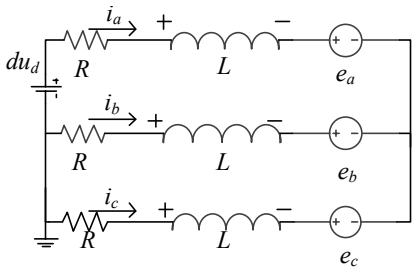

(a) S_b^-turn on

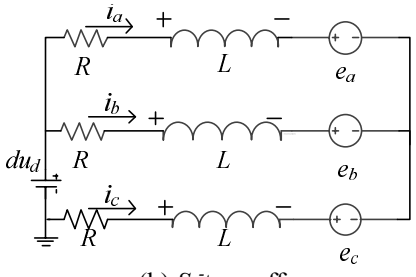

(b) S_b^-turn off

Fig.4. Equivalent circuit of S_b^- turned on and off

The equivalent circuit diagram of the three-phase winding conduction can be obtained [Figs. 4(a) and (b)] by analyzing the three-phase winding conduction in Figs. 3(a) and (b).

According to Kirchhoff's law, Fig. 4(a) can be written as a phase voltage equation for three-phase winding, as follows:

$$\begin{cases} u_a = Ri_a + L\dfrac{di_a}{dt} + e_a + u_N = d \cdot u_d \\ u_b = Ri_b + L\dfrac{di_b}{dt} + e_b + u_N = 0 \\ u_c = Ri_c + L\dfrac{di_c}{dt} + e_c + u_N = 0 \end{cases} \tag{2}$$

where u_d is the bus voltage.

When S_b^- is conducting, i_b and i_c current responses can be expressed by Eq. (2), as follows:

$$\begin{aligned} Ri_b + L\frac{di_b}{dt} &= \frac{2E - d \cdot u_d}{3} = u_{b1} \\ Ri_c + L\frac{di_c}{dt} &= \frac{2E - d \cdot u_d}{3} = u_{c1} \end{aligned} \tag{3}$$

When the commutation signal of the BLDCM is detected, the three-phase winding is i_b=-I and i_c=0. The initial value of the current is shown in Eq. (3). Thus, the phase winding currents of *b* and *c* can be calculated as follows:

$$\begin{cases} i_{b1} = \dfrac{u_{b1}}{R} + \left(-I - \dfrac{u_{b1}}{R}\right) e^{-\frac{R}{L}t} \\ i_{c1} = \dfrac{u_{c1}}{R} - \dfrac{u_{c1}}{R} e^{-\frac{R}{L}t} \end{cases} \tag{4}$$

where $u_{b1} = u_{c1} = \dfrac{2E - d \cdot u_d}{3}$.

Eq. (4) is expressed as a Taylor expansion, ignoring terms higher than the second-order terms. Thus, $e^{-(R/L)t} = 1 - (R/L) \cdot t$. The simplified i_{b1} and i_{c1} terms are shown in Eq. (5), as follows:

$$\begin{cases} i_{b1} = -I + \dfrac{u_{b1} + IR}{L} t \\ i_{c1} = \dfrac{u_{c1}}{L} t \end{cases} \tag{5}$$

From Eq. (5), i_{b1} is changed from $-I$ zero, using the slope of $\frac{IR+u_{b1}}{L}$ during commutation.

When analyzing S_b^- disconnected, still use the above method, but the initial values of i_{b2} and i_{c2} are changed. After S_b^- is opened for $T_s \cdot d_{off}$ period of time, changes in i_{b2} and i_{c2} current can be obtained as follows:

$$\begin{aligned} i_{b2}\left(T_s \cdot d_{off}\right) &= -I + \frac{u_{b1}+IR}{L}\left(T_s \cdot d_{off}\right) \\ i_{c2}\left(T_s \cdot d_{off}\right) &= \frac{u_{c1}}{L}\left(T_s \cdot d_{off}\right) \end{aligned} \tag{6}$$

When S_b^- is opened, the i_{b2} and i_{c2} responses of the BLDCM are similar when S_b^- is off, the following equation can shows:

$$\begin{cases} i_{b2} = i_{b2}^*(0) + \dfrac{u_{b2}+i_{b2}^*(0)R}{L}t \\ i_{c2} = i_{c2}^*(0) + \dfrac{u_{c2}+i_{c2}^*(0)R}{L}t \end{cases} \tag{7}$$

where： $u_{b2} = \frac{2E+du_d}{3}$, $u_{c2} = \frac{2E-2du_d}{3}$

$i_{b2}^*(0) = i_{b2}\left(T_s \cdot d_{off}\right)$, $i_{c2}^*(0) = i_{c2}\left(T_s \cdot d_{off}\right)$

In BLDCM commutation, the decline in the rate of i_b and increase in the rate of i_c can be expressed as follows:

$$\begin{aligned} k_{i_b} &= k_{i_{b1}} \times d_{off} + k_{i_{b2}} \times \left(1-d_{off}\right) \\ &= \frac{\left(2E+du_d+3IR\right)\cdot L - \left(2E-du_d+3IR\right)\cdot\left(T_s \cdot d_{off}\right)\cdot R}{3L^2} \\ &+ \left[\frac{-2du_d \cdot L + \left(2E-du_d+3IR\right)\cdot\left(T_s \cdot d_{off}\right)\cdot R}{3L^2}\right]\cdot d_{off} \\ k_{i_c} &= k_{i_{c1}} \times d_{off} + k_{i_{c2}} \times \left(1-d_{off}\right) \\ &= \frac{\left(2E-2du_d\right)\cdot L - \left(2E-du_d\right)\cdot\left(T_s \cdot d_{off}\right)\cdot R}{3L^2} \\ &+ \left[\frac{du_d \cdot L - \left(2E-du_d\right)\cdot\left(T_s \cdot d_{off}\right)\cdot R}{3L^2}\right]\cdot d_{off} \end{aligned} \tag{8}$$

Bus voltage is modulated by the duty cycle d and satisfy the following equation:

$$du_d = 2\left(IR+E\right) \tag{9}$$

Therefore, k_{ib} and k_{ic} can be simplified, as follows:

$$k_{i_b} = \frac{IR^2T_s \cdot d_{off}^2 - \left(IR^2T_s + 2du_d \cdot L\right)\cdot d_{off} + \left(2du_d + IR\right)\cdot L}{3L^2}$$

$$k_{i_c} = \frac{2IR^2T_s \cdot d_{off}^2 + \left(2IR^2T_s + du_d \cdot L\right)\cdot d_{off} - \left(du_d + 2IR\right)\cdot L}{3L^2} \tag{10}$$

Eq. (10) shows that adjusting the off-phase duty cycle can not only slow down the decline of the current during the turned-off-phase, but also can speed up the increase in current during conduction. Thus, the commutation torque ripple can be reduced and commutation time can be shortened simultaneously. This method shortens the uncontrollable time of motor commutation, making the method more suitable for motor working at high-speed.

The generation of the commutation torque ripple in a BLDCM is primarily caused by the difference in the decline and increasing rates of the currents during the off and conduction phases, respectively. The torque ripple is eliminated when the decline rate of i_b and increase rate of i_c are consistent, that is, $k_{ib}=-k_{ic}$. This characteristic can also be expressed as follows:

$$3IR^2T_s \cdot d_{off}^2 + \left(IR^2T_s - du_d \cdot L\right)\cdot d_{off} + \left(du_d - IR\right)\cdot L = 0 \tag{11}$$

In a BLDCM control system, the PWM period T_s is typically a few microseconds. Thus, this parameter has little effect on the control method. Therefore, the paper ignore T_s, and Eq. (11) can also be expressed as follows:

$$-du_d \cdot L \cdot d_{off} + \left(du_d - IR\right)\cdot L = 0 \tag{12}$$

Solving Eq. (12), the duty d_{off} during the off-phase can be expressed as follows:

$$d_{off} = 1 - \frac{IR}{dU_d} \tag{13}$$

2.4 Calculation of commutation time

When motor commutation is completed, the current during shutdown drops to zero. Then, the current during conduction increases to its maximum value. Thus, the rates of change in the current during conduction and shutdown become consistent. The phase current is assumed to drop to zero, and commutation time is calculated.

During commutation, changes in the i_b current satisfy the following relationship:

$$i_b = -I + k_{i_b}t \tag{14}$$

When i_b=0, the commutation time can be expressed as follows:

$$T = \frac{3IL^2}{IR^2T_s \cdot d_{off}^2 - \left(IR^2T_s + 2du_d \cdot L\right)\cdot d_{off} + \left(2du_d + IR\right)\cdot L} \tag{15}$$

3. Simulation and Analysis

The method for inhibiting the commutation torque ripple in a BLDCM is validated. The simulation models, namely, permanent magnet synchronous motor (PMSM), speed control module and commutation control module, in Matlab / Simulink environment is established in this paper.

In this simulation system, the PMSM counter EMF is a trapezoidal back EMF. The commutation control module detects the back EMF and controls the universal bridge to modulate the duty cycle during conduction. When the speed control module detects the commutation time, the commutation control module triggers the torque control module. In the commutation control module, the module reads the DC link current and bus voltage, calculates the duty cycle when shutdown, and suppresses the current ripple at the non-commutation phase. The module also calculates the commutation time. When the commutation time has been determined, the commutation torque ripple control is terminated. At the end of the commutation process, the speed control module controls the speed of the BLDCM system according to the duty cycle calculated by the speed PID unit.

The phase current and torque waveforms of the three-phase winding of a BLDCM with load is shown in Figs. 5 and 6. During any of the commutation phases, the rates of changes in current during conduction and shutdown are inconsistent. This characteristic leads to a current ripple in the non-commutation phase and electromagnetic torque fluctuations during commutation.

Amplified waveforms of three-phase winding phase current when no torque ripple control is applied are shown in Fig. 7. During commutation, three-phase winding phase i_b drops down to zero, but the conduction phase i_a does not increase to its maximum value, resulting in significantly lower increase rate in current during conduction than the decrease rate in current during shutdown. However, the summation of the three phase currents is zero at any time, which inevitably leads to the current ripple during the non-commutation phase.

Fig. 8 shows the waveform diagram of the electromagnetic torque during commutation. The back EMF during commutation is approximately constant. Thus, the speed mutation during commutation, and the current ripple during the non-commutation phase will inevitably lead to the commutation torque ripple.

The waveform of the three-phase winding phase current when the proposed commutation torque ripple control method is applied is shown in Fig. 9. After application of the proposed control method, the increase rate in current

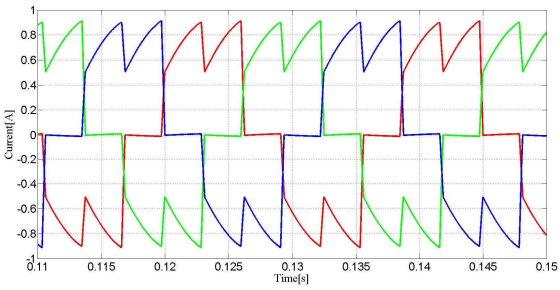

Fig. 5. Phase current waveforms without torque ripple control

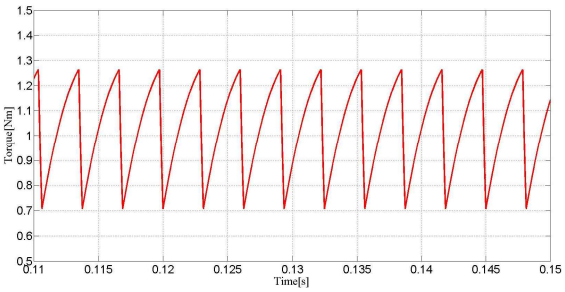

Fig. 6. Electromagnetic torque waveforms without torque ripple control

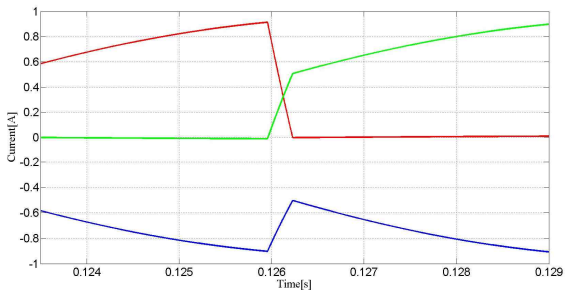

Fig. 7. Simulation results of the phase current without torque ripple control

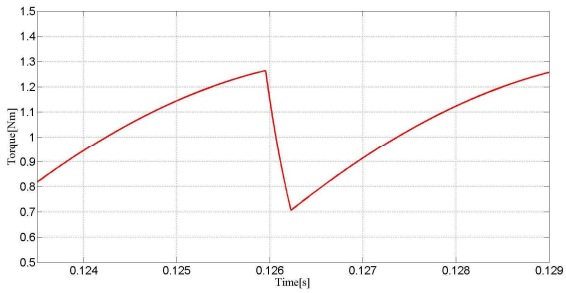

Fig. 8. Simulation results of the electromagnetic torque without torque ripple control

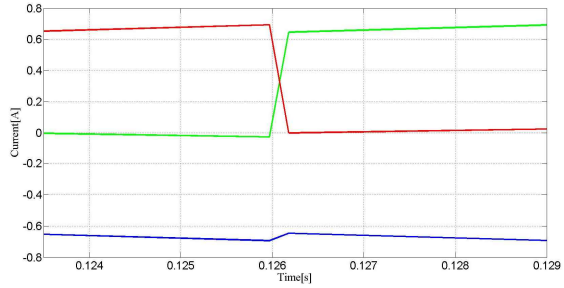

Fig. 9. Simulation results of phase current with torque ripple control

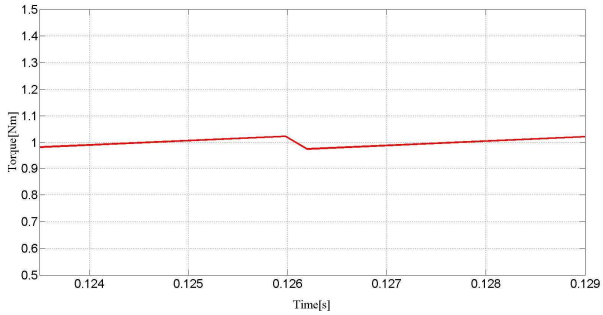

Fig. 10. Simulation results of electromagnetic torque with torque ripple control

Table 1. Phase current simulation results

	Current		Torque	
	Without	With	Without	With
Min	0.5047	0.6462	0.7093	0.9582
Max	0.9028	0.694	1.2642	1.0191
RF	56.9%	6.8%	55.5%	6.09%

during conduction is significantly higher than that without the proposed control method. After commutation, the phase current almost increases to its maximum value, so the pulse during the non-commutation phase of BLDCM is significantly reduced. The electromagnetic torque waveform when the proposed control method is used is shown in Fig. 10. During commutation, the BLDCM commutates smoothly with almost no torque ripple.

The suppression of the commutation torque ripple using the proposed method is quantitatively analyzed using the following equation to calculate key ripple factor (RF) parameters.

$$\Delta X = \frac{X_{\max} - X_{\min}}{X_{av}} \tag{16}$$

where ΔX is the parameter RF, and X_{max}, X_{min}, and X_{av} are the maximum, minimum, and average values of parameter X.

The key parameters of the simulation results are shown in Table 1.

Table 1 shows that, compared with the phase current and torque without torque control method, the proposed method can effectively suppress the current and commutation torque ripple during the non-commutation phase.

Simulation results show that the proposed method can not only retard the decrease in current during shutdown but can also effectively improve the increase in current during conduction. This process guarantees the consistency of the rates of change in the currents during shutdown and conduction during commutation. This method can effectively reduce the current ripple of the non-commutation phase, thereby inhibiting the commutation torque ripple. Thus, the simulation results demonstrate the feasibility of the proposed method.

4. Experimental Verification

To verify the feasibility of the method, a control platform using TMS320F2812 as the master chip, IRF2807 MOSFET as a three-phase full-bridge power device, IR2136S as power devices driver chip, and Hall current sensors to measure the bus current was established. The experimental prototype is a BLDCM with four pairs of poles and a star connection. Its parameters are as follows: rated DC voltage u_d, 24V; rated torque T_N, 0.18 Nm; rated speed n, 2000 rpm; phase resistance R, 1.2 Ω; and effective inductance L, 1.2 mH.

When the control system detects the commutation signals, the motor immediately initiates the commutation control process. The controller calculates the duty cycle and commutation time of the off-phase. When the running and commutation times are equal, the controller exits the commutation control, and the motor cuts back the PWM-ON speed control mode.

To verify the proposed method not only in the high-speed region but also in the low-speed region with good phase current ripple suppression. The paper conducts experiments in the low-speed (800 rpm) and high-speed (2000 rpm) areas.

Fig. 1 shows that the waveforms of the three phase currents in a BLDCM winding are similar, and these waveforms only differ in phases, that is, 120°. To simplify the analysis, the paper only analyze a phase winding to elucidate the causes of the ripple in the phase current of a BLDCM.

Fig. 11(a) is the phase current waveform of the BLDCM with traditional method, in which the upper arm uses PWM speed control, and the lower arm uses regular conduction control. The rotation speed is 800 rpm, load torque is 0.05 Nm, and the duty cycle d is 0.4. The non-commutation phase current i_a rapidly declines during commutation. During this time, the speed and the counter EMF E_a can be considered constant. Therefore, the rapid decline in the phase current reduces torque ripple. The current waveform diagram when the proposed control method is used to control a BLDCM is shown in Fig. 11(b).

Comparing Figs. 11(a) and 11(b) it can be shown that the smaller slope of the phase current during the increase and decrease in current when the proposed method is used compared with that when traditional control methods are used. This phenomenon is due to the additional commutation control strategy, which adjusts the rate of change in the phase current to ensure less current pulse during the non-commutation phase. In Fig. 11(b), the non-commutation phase current is running smoothly when the BLDCM commutates, and almost no commutation fluctuation occurs. This phenomenon indicates that the commutation torque ripple is suppressed.

In order to provide a better illustration of the proposed method, the amplified waveforms are shown in Figs. 12(a) and (b). During commutation, the phase current ripple factors are significantly reduced, and commutation is more stable. The experimental results showed that the proposed method can be applied in the low-speed zone.

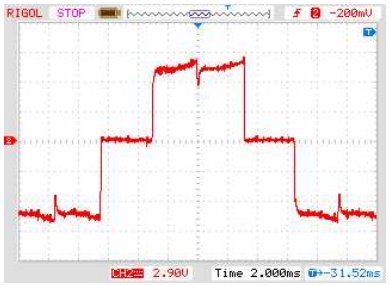

(a)

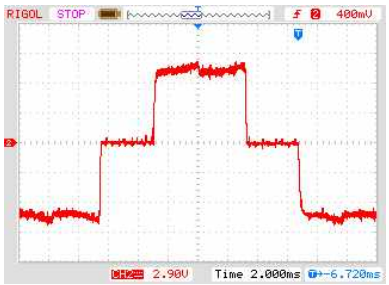

(b)

Fig. 11. Current fluctuation waveforms at 800 rpm (a) without and (b) with the proposed commutation control strategy

(a)

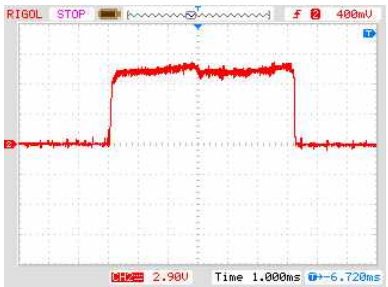

(b)

Fig. 12. Amplified current fluctuation waveforms at 800 rpm (a) without and (b) with the proposed commutation control strategy

Figs. 13 show the changes in the motor phase current under the same motor load as that in Fig. 11 but at rotational speed of 2000 rpm. The current waveforms of the phase current without and with commutation control strategy are shown in Figs. 13(a) and (b), respectively.

Figs. 13(a) and (b) are partially amplified, and the results

(a)

(b)

Fig. 13. Current fluctuation waveform of 2000 rpm(a) without and (b) with the proposed commutation control strategy

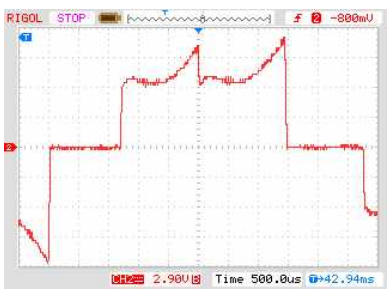

(a)

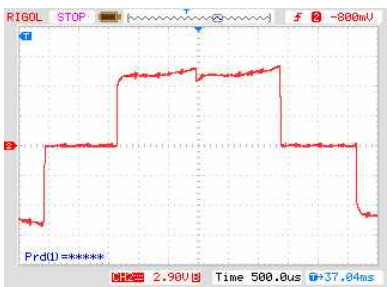

(b)

Fig. 14. Amplified current fluctuation waveform at 2000 rpm (a) without and (b) with the proposed commutation control strategy

are shown in Figs. 14 (a) and (b).

Fig. 14(a) shows that, the current ripple during commutation is higher when the speed is 2000 rpm than at 800 rpm. This condition increases the torque ripple compared with that when traditional control method is applied in the high-speed zone.

Using the proposed method, The paper let the motor run under the same load torque, and the phase current ripple is shown in Fig. 13(b). The proposed method significantly reduced commutation torque ripple compared with the traditional speed control method.

The magnitude of the phase current ripple of the BLDCM during commutation can be obtained using Figs. 14. The phase current RF is calculated by Eq. (16), and the results are shown in Table 2.

Table 2. Phase current ripple results

	800r/min		2000r/min	
	Without	With	Without	With
Min	0.534	0.667	0.609	0.618
Max	0.812	0.783	0.986	0.754
RF	40.0%	16.7%	50.0%	18.8%

Table 2 shows that the proposed control method can inhibit the phase current ripple in the low-speed and high-speed zones.

The experimental results show that the proposed method can significantly control the current ripple during the non-commutation phase of a BLDCM to a level lower than that when a traditional control method is used. In particular, the inhibitory effect is more evident in the high-speed range. The motor works stably at both zones when the proposed method is applied, indicating that the method has strong adaptability and reliability.

5. Conclusion

This paper proposed a new commutation current control method to control the torque ripple in a BLDCM during commutation, and considered the armature resistance in the proposed method. The "open-phase conduction, off-phase pulse width modulation, and non-commutation phase" modulation method was used during commutation. The rate of change in the current was made to be equal during commutation by controlling the duty cycle. Thus, This paper established and analyzed the mathematical model of the three-phase current during commutation. This process ensured a constant current during non-commutation, thereby reduced the commutation torque ripple.

Compared with other methods that suppress the torque ripple in BLDCMs, the proposed method exhibits the following advantages:

a) The proposed method showed higher accuracy in controlling the ripple of the phase current, because the impact of armature resistance to the phase current during commutation is considered.

b) No additional hardware is required, but CPU performance requirements are reduced, because the calculation of the off duty cycle and phase commutation time does not depend on the phase current and back-EMF.

c) The method can be used in low and high ranges, eliminating the need to distinguish these two zones in the inhibition of the phase current ripple.

References

[1] E Bostanci, Z Neuschl, R Plikat, B Ponick, "No-Load Performance Analysis of Brushless DC Machines With Axially Displaceable Rotor," *IEEE Transactions on Industrial Electronics*, 2014. vol. 61, no. 4, pp. 1692-1699.

[2] SY Jung, YJ Kim, J Jae, J Kim, "Commutation Control for the Low-Commutation Torque Ripple in the Position Sensorless Drive of the Low-Voltage Brushless DC Motor," *IEEE Nactions on Power Electronics*, 2014. vol. 29, no. 11, pp. 5983-5994.

[3] Gundogdu, T. and G. Komurgoz, "Self-Tuning PID Control of a Brushless DC Motor by Adaptive Interaction," *IEEJ Transactions on Electrical & Electronic Engineering*, 2014. vol. 9, no. 4, pp. 384-390.

[4] Z Li, S Zhang, S Zhou, JW Ahn, "Torque Ripple Minimization in Direct Torque Control of Brushless DC Motor," *Journal Of Electrical Engineering & Technology*, 2014. vol. 9, no. 5, pp. 1569-1576.

[5] Masmoudi, M., B. El Badsi, A. Masmoudi, "DTC of B4-Inverter-Fed BLDC Motor Drives With Reduced Torque Ripple During Sector-to-Sector Commutations," *IEEE Transactions on Power Electronics*, 2014. vol. 29, no. 9, pp. 4855-4865.

[6] M Masmoudi, BE Badsi, A Masmoudi, "Analysis and Mitigation of Torsional Vibration of PM Brushless AC/DC Drives With Direct Torque Controller," *IEEE Transactions on Industry Applications*, 2012. vol. 48, no. 4, pp. 1296-1306.

[7] Y. Liu, ZQ Zhu, D. Howe, "Commutation-Torque-Ripple Minimization in Direct-Torque-Controlled PM Brushless DC Drives," *IEEE Transactions on Industry Applications*, 2007. vol. 43, no. 4, pp. 1012-1021.

[8] Ozturk, S.B. and H.A. Toliyat, "Direct Torque and Indirect Flux Control of Brushless DC Motor," *IEEE/ASME Transactions on Mechatronics*, 2011. vol. 16, no. 2, pp. 351-360.

[9] C. Xia, Y. Xiao, W. Chen, T. Shi, "Torque Ripple Reduction in Brushless DC Drives Based on Reference Current Optimization Using Integral Variable Structure Control," *IEEE Transactions on Industrial Electronics*, 2014. vol. 61, no. 2, pp. 738-752.

[10] Xia, C., Y. Wang, and T. Shi, "Implementation of Finite-State Model Predictive Control for Commutation Torque Ripple Minimization of Permanent-Magnet Brushless DC Motor," *IEEE Transactions on Industrial Electronics*, 2013. vol. 60, no. 3, pp. 896-905.
[11] Preindl, M., E. Schaltz, and P. Thogersen, "Switching Frequency Reduction Using Model Predictive Direct Current Control for High-Power Voltage Source Inverters," *IEEE Transactions on Industrial Electronics*, 2011. vol. 58, no. 7, pp. 2826-2835.
[12] P Cortes, J Rodriguez, C Silva, A Flores, "Delay Compensation in Model Predictive Current Control of a Three-Phase Inverter," *IEEE Transactions on Industrial Electronics*, 2012. vol. 59, no. 2, pp. 1323-1325.
[13] Lu, H.F., L. Zhang, and W.L. Qu, "A New Torque Control Method for Torque Ripple Minimization of BLDC Motors With Un-Ideal Back EMF," *IEEE Transactions on Power Electronics*, 2008. 23(2): p. 950-958.
[14] Fang, J., H. Li, and B. Han, "Torque Ripple Reduction in BLDC Torque Motor With Nonideal Back EMF," *IEEE Transactions on Power Electronics*, 2012. vol. 27, no. 11, pp. 4630-4637.
[15] Carlson R, Lajoie-Mazenc M, Fagundes J C D S, "Analysis of Torque Ripple Due to Phase Commutation in Brushless DC Machines," *IEEE Transactions on Industry Applications*, 1992. vol. 28, no. 3, pp. 632-638.
[16] Song, J.H. and I. Choy, "Commutation Torque Ripple Reduction in Brushless DC Motor Drives Using a Single DC Current Sensor," *IEEE Transactions on Power Electronics*, 2004. vol. 19, no. 2, pp. 312-319.
[17] Shi, X. and S. Chang, "Commutation Force Ripple Reduction in a Novel Linear Brushless DC Actuator Based on Predictive Current Control," *Electric Power Components & Systems*, 2011. vol. 39, no. 15, pp. 1609-1620.
[18] K.Y. Nam, W. T. Lee, C. M. Lee, J. P. Hong, "Reducing Torque Ripple of Brushless DC Motor by Varying Input Voltage," *IEEE Transactions on Magnetics*, 2006. vol. 42, no. 4, pp. 1307-1310.
[19] Lin, Y.-K. and Y.-S. Lai, "Pulsewidth Modulation Technique for BLDCM Drives to Reduce Commutation Torque Ripple Without Calculation of Commutation Time," *IEEE Transactions on Industry Applications*, 2011. vol. 47, no. 4, pp. 1786-1793.
[20] Ho, Z. S., C. M. Uang, and P. C. Wang, "Extracting DC Bus Current Information for Optimal Phase Correction and Current Ripple in Sensorless Brushless DC Motor Drive," *Journal of Zhejiang University-Science C-Computers & Electronics*, 2014. vol. 15, no. 4, pp. 312-320.
[21] Viswanathan, V. and S. Jeevananthan, "A Novel Space-Vector Current Control Method for Commutation Torque Ripple Reduction of Brushless DC Motor Drive," *Arabian Journal for Science and Engineering*, 2013. vol. 38, no. 10, pp. 2773-2784.
[22] T Shi, Y Guo, P Song, C Xia, "A New Approach of Minimizing Commutation Torque Ripple for Brushless DC Motor Based on DC-DC Converter," *IEEE Transactions on Industrial Electronics*, 2010. vol. 57, no. 10, pp. 3483-3490.
[23] Shi, J. and L.T. Cai, "New Method to Eliminate Commutation Torque Ripple of Brushless DC Motor With Minimum Commutation Time," *IEEE Transactions on Industrial Electronics*, 2013. vol. 60, no. 6, pp. 2139-2146.

Zhiqiang Wang received Bachelor's degree in Mechanical Design manufacture and Automation Major from the North University of China, 2011. At present, he is working on his Ph.D. course in Instrumentation Science and Technology from the North University of China. His research interests include electrical machines and power electronics.

Shuai Yin received Ph.D. degree in Instrument Science and technology from the North University of China, 2017. At present, he is working at the college of mechanical engineering at Zaozhuang University. His research interests include electrical machines and motor drives, and modeling optimization of electrical machines.

Tiehua Ma received the Ph.D. degree in Nanjing University of Science and Technology in 1990. He has been a visiting scholar at the University of LSU, USA, in 2002, and 2003. He is working as a Professor in North University of China, and also a director of the National Key Laboratory of Electronic Measurement. His research interests include dynamic test and intelligent control.